MEASUREMENTS OF π^-p FORWARD ELASTIC SCATTERING AT HIGH ENERGIES

J.P. Burq*), M. Chemarin*), M. Chevallier*), A.S. Denisov**),
 T. Ekelöf***,+), J. Fay*). P. Grafström***,+), L. Gustafsson+),
 E. Hagberg+), B. Ille*), A.P. Kashchuk**), A.V. Kulikov**),
 M. Lambert*), J.P. Martin***,*), S. Maury***,++), M. Querrou++),
 V.A. Schegelsky**), I.I. Tkach**), M. Verbeken++) and A.A. Vorobyov**)

ABSTRACT

The differential cross-section of π^-p scattering has been measured in the energy region 100 - 345 GeV and in the t -range $0.002 < |t| < 0.04$ (GeV/c)². The real part of the π^-p scattering amplitude has been extracted from the data. The results show that the real part continues to increase with energy. The energy dependence of the slope parameter has also been determined. The shrinkage found expressed in terms of the slope of the Pomeron trajectory is $2\alpha'_p = 0.23 \pm 0.04$ (GeV/c)⁻². This agrees with the energy dependence found at larger $|t|$ -values.

submitted to Physics Letters B

-
- *) Institut de Physique Nucléaire, IN2P3, Université de Lyon-Villeurbanne, France.
 - **) Leningrad Nuclear Physics Institute, Gatchina, USSR.
 - ***) At present, CERN, Geneva, Switzerland.
 - +) The Gustaf Werner Institute, University of Uppsala, Sweden.
 - ++) Laboratoire de Physique Corpusculaire, IN2P3, Université de Clermont-Ferrand, Aubière, France.

In a recently finished experimental program performed at the CERN SPS the π^-p elastic scattering cross-section has been measured in the energy region 100 - 345 GeV and in the t -range $0.002 < |t| < 0.04$ (GeV/c)². The experimental method employed in this experiment is essentially the same as used in our previous experiment [1] investigating the energy range 30 - 140 GeV. The recoil detector, an ionization chamber filled with 10 atm. H₂, measured the kinetic energy and the polar angle of the recoil. The t -resolution in the Coulomb interference region was $\Delta t \approx 10^{-4}$ (GeV/c)². The scattering angle and the momentum of the forward scattered particle was measured using a MWPC-magnet spectrometer. The absolute momentum of the beam particles was measured with a high resolution beam spectrometer, to a precision of .15% [2]. For identification of the incident hadrons, two differential Cerenkov counters and two threshold Cerenkov counters were used. An electromagnetic shower detector was used to eliminate electrons in the beam. Muons were identified with the aid of two scintillation counters placed behind a beam stopper of 4 m iron. Details about the experimental layout can be found in ref. [3]. The trigger system included a special fast processor which selected events scattered by angles bigger than some preset values. Precautions were made to include in the trigger also those elastic events which might be accompanied by bremsstrahlung gammas.

After having eliminated obvious background by rough cuts in a first stage analysis, the elastic events were selected using the kinematical correlations between the forward scattering angle, the recoil energy and the recoil polar angle. The corrections for background were typically 1-2%. These corrections as well as corrections made to account for the detection inefficiency of different parts of the detector system were determined experimentally using test signals sent to the recoil detector in coincidence with signals from a real incident particle [3]. The measured detection inefficiency was found to be $\sim 10\%$. The overall correction for background and for inefficiency was measured with an estimated accuracy of better than 1%. The effective thickness of the target was measured with a precision of $\pm 0.3\%$. This made it possible to determine the absolute differential cross-sections with normalization uncertainty of $\pm 1\%$. The t -scale was calibrated experimentally [2] to a precision better than 0.5% throughout the t -range under investigation. Some elastic events

accompanied by bremsstrahlung were lost in the analysis due to the application of a momentum cut. Thus particles having a difference between incoming and outgoing momentum larger than 5% of the incoming momentum were rejected. The measured cross-section was corrected for this loss [4]. As an example, the differential cross-section of π^-p scattering at 300 GeV is shown in Fig. 1.

The differential cross-sections have been fitted with the following parametrization:

$$\frac{d\sigma}{dt} = K \left\{ \frac{4\pi\alpha^2\hbar^2}{\beta^2|t|^2} G_\pi^2 G_p^2 + (1 + \rho^2) \frac{\sigma_{\pi-p}^2}{16\pi\hbar^2} e^{-b|t|} + \right. \\ \left. + \frac{\sigma_{\pi-p}}{\beta|t|} \alpha (-\sin \delta + \rho \cos \delta) e^{-b|t|/2} G_\pi G_p \right\} \text{mb}/(\text{GeV}/c)^2 \quad (1)$$

where K is the normalization parameter; α is the fine structure constant (1/137); β is the velocity of the incident particle; $\sigma_{\pi-p}$ is the total hadronic cross-section (mb); ρ is the ratio of the real to imaginary parts of the forward elastic scattering amplitude; b is the logarithmic slope of the differential hadronic elastic cross-section ((GeV/c)⁻²); $G_\pi = (1 + |t|/0.59)^{-1}$ and $G_p = (1 + |t|/0.71)^{-2}$ are the electromagnetic form factors of the pion and the proton, respectively [5]; $\delta = -[\ln(|t|/0.092 + 0.577)] \cdot \alpha/\beta$ is the Bethe phase [6]; and $\hbar = 0.624 \text{ GeV} \cdot \sqrt{\text{mb}}$. The normalization parameter K was constrained to be equal to unity with a standard deviation of $\pm 1\%$. Data from the total cross-section measurements of Carroll et al. [7] were used to constrain the values of $\sigma_{\pi-p}$.

The results of the fits are given in Table 1. The errors given include statistical errors, the quoted error in the normalization parameter and the errors in $\sigma_{\pi-p}$ as given in Ref. [7]. The fitted value of K was always unity within the one standard deviation limit. A shift of the $\sigma_{\pi-p}$ values of +0.1 mb would shift the ρ -values by -0.004. Fixing the b values and using only the lower |t| region ($|t| < 0.009 \text{ (GeV}/c)^2$) gives $d\rho/db = 0.003 \text{ (GeV}/c)^2$.

The real part is related to the total cross-section through dispersion relations. This can be used to get a glimpse of the energy dependence of the total cross-section at higher energies not accessible for measurements today. We have compared our results with the dispersion relation

prediction of Höhler et al., [8]. This calculation is the only one known to us which uses a parametrization of the total cross section that takes into account and describes well the recent total cross section data of Carroll et al., [7]. For the asymptotic behaviour, Höhler et al. assumes a rise of the total cross section of the form

$$\sigma_{\infty} \propto \sigma_1 \ln^2 p/p_1 \quad (2)$$

where $\sigma_1 = 0.42$ mb; $p_1 = 38$ GeV/c and p is the momentum in the laboratory system. From fig. 2 is seen that our measured ρ -values are systematically below the dispersion relation prediction indicating that the total cross section at high energies rises more slowly than suggested by (2). Details of a simultaneous fit to ρ and σ_{tot} data with the aim to obtain more information about the high energy behaviour of the total cross section will be published in a forthcoming article.

The values of the slope parameter b obtained are given in Table 1 and in Fig. 3. The data available from other experiments in the t -region close to $t = 0$ are also shown in the figure. Our data and the data of Fajardo et al. [10] in the energy range 70-200 GeV agrees reasonably well. Our previous published results in the energy range 30 - 140 GeV have been corrected by $\Delta b = -0.5$ (GeV/c)⁻². This change is due to the introduction of radiative corrections and of an efficiency correction at big t -values which was neglected in the previous analysis. From the b -data of Foley et al. [11] we have included only those energy points for which the measurements of ρ are consistent with the values given by dispersion relation. Values of ρ obtained from dispersion relation calculation at these low energies (< 30 GeV) are quite accurately determined by already measured total cross sections and we have therefore imposed this consistency condition on the data in particular as there is a correlation between ρ and b when fitting the data. In the experiment of Russ et al. [12] the minimum t -value is $|t| = 0.05$ (GeV/c)². We have extrapolated to $|t| = 0.02$ (GeV/c)² using the t -dependence suggested by the authors.

We have also compared our results on the slope parameter with the measurements at larger $|t|$ -values. Figure 3 shows our compilation of the world data at $|t| = 0.2$ (GeV/c)² and $|t| = 0.4$ (GeV/c)². Details of this compilation will be published elsewhere.

The following parametrization suggested by classical Pomeron theory: has been fitted to the data of fig. 3 for each $|t|$ -value separately;

$$b(p) = b_0 + 2\alpha'_p \ln p \quad (3)$$

where p is the momentum of the incident particle and α'_p the slope of the Pomeron trajectory. From the results of these fits shown in fig. 3 we conclude that there is shrinkage at all three $|t|$ -values, and that within the error bars the shrinkage parameter is independent of t , the average value being $2\alpha'_p \approx 0.21 \text{ (GeV/c)}^{-2}$. Furthermore, the decrease in b between $|t| = .02 \text{ (GeV/c)}^2$ and $|t| = .2 \text{ (GeV/c)}^2$ is significantly larger than the decrease between $|t| = .2 \text{ (GeV/c)}^2$ and $|t| = .4 \text{ (GeV/c)}^2$, implying a non linear variation of b with t in this t -range. The latter statement agrees with the conclusion of Schiz et al., where the t -dependence of the slope parameter was measured at 200 GeV/c [13].

Table 1

Values of ρ and b for π^-p scattering as determined in the fits

Energy (GeV)	No. of events	$\sigma_{\text{tot}} \pm \Delta\sigma$ from Ref. 7 (mb)	$\rho \pm \Delta\rho$	$b \pm \Delta b$ (GeV/c) ⁻²	χ^2/NDF
100	100,000	24.00 \pm .06	.048 \pm .012	10.54 \pm .31	80/69
150	130,000	24.11 \pm .04	.048 \pm .012	10.09 \pm .28	54/64
200	140,000	24.34 \pm .04	.064 \pm .011	10.30 \pm .27	67/61
250	80,000	24.65 \pm .05	.078 \pm .013	10.39 \pm .31	51/55
280	115,000	24.76 \pm .06	.087 \pm .012	10.51 \pm .29	62/53
300	150,000	24.86 \pm .08	.090 \pm .012	10.73 \pm .29	48/55
325	120,000	24.99 \pm .08	.084 \pm .012	10.90 \pm .30	78/52
345	110,000	25.11 \pm .08	.075 \pm .012	11.03 \pm .31	66/53

REFERENCES

- [1] J.P. Burq et al., Phys. Lett., 77B (1978) 438.
- [2] J.P. Burq et al., Nucl. Instr. Meth., 177 (1980) 353.
- [3] J.P. Burq et al., Nucl. Phys., B187 (1981) 205.
- [4] M. Sogard, Phys. Rev., D9 (1974) 1486.
- [5] M.M. Nagels et al., Nucl. Phys., B109 (1976) 1.
- [6] G.B. West and D.R. Yennie, Phys. Rev., 172 (1968) 1413.
- [7] A.S. Carroll et al., Phys. Lett., 80B (1979) 423.
- [8] G. Höhler, to be published in Volume 9b, series 1, Landolt-Bernstein.
- [9] V.D. Apokin et al., Ya. Fiz., 28 (1978) 1529.
- [10] L.A. Fajardo et al., Phys. Rev., D24 (1981) 46.
- [11] K.J. Foley et al., Phys. Rev., 181 (1969) 1775.
- [12] J.S. Russ et al., Phys. Rev., D15 (1977) 3139.
- [13] A. Schiz et al., Phys. Rev., D24 (1981) 26.

Figure captions

- Fig. 1 : The measured differential cross-section at 300 GeV. The full curves result from the fit mentioned in the text. The dot-dashed line represents the $\rho = 0$ curve for comparison. The dashed line in the lower plot shows the hadronic amplitude squared plotted up to the optical point.
- Fig. 2 : Experimental data on ρ for π^-p scattering. The full line represents ρ calculated using dispersion relations and the parametrization of σ_{tot} suggested by Höhler et al. [8].
- Fig. 3 : The slope parameter b at different t -values as a function of incident momentum. The points at $|t| = 0.2 \text{ (GeV/c)}^2$ and $|t| = 0.4 \text{ (GeV/c)}^2$ represents our compilation of the world data. The full lines represent a fit to the data with the parametrization $b_0 + 2\alpha'_p \ln p$. The values of $2\alpha'_p$ found were $0.23 \pm 0.04 \text{ (GeV/c)}^{-2}$, $0.22 \pm 0.02 \text{ (GeV/c)}^{-2}$ and $0.19 \pm 0.03 \text{ (GeV/c)}^{-2}$ at $|t| = 0.02 \text{ (GeV/c)}^2$, $|t| = 0.2 \text{ (GeV/c)}^2$ and $|t| = 0.4 \text{ (GeV/c)}^2$ respectively.

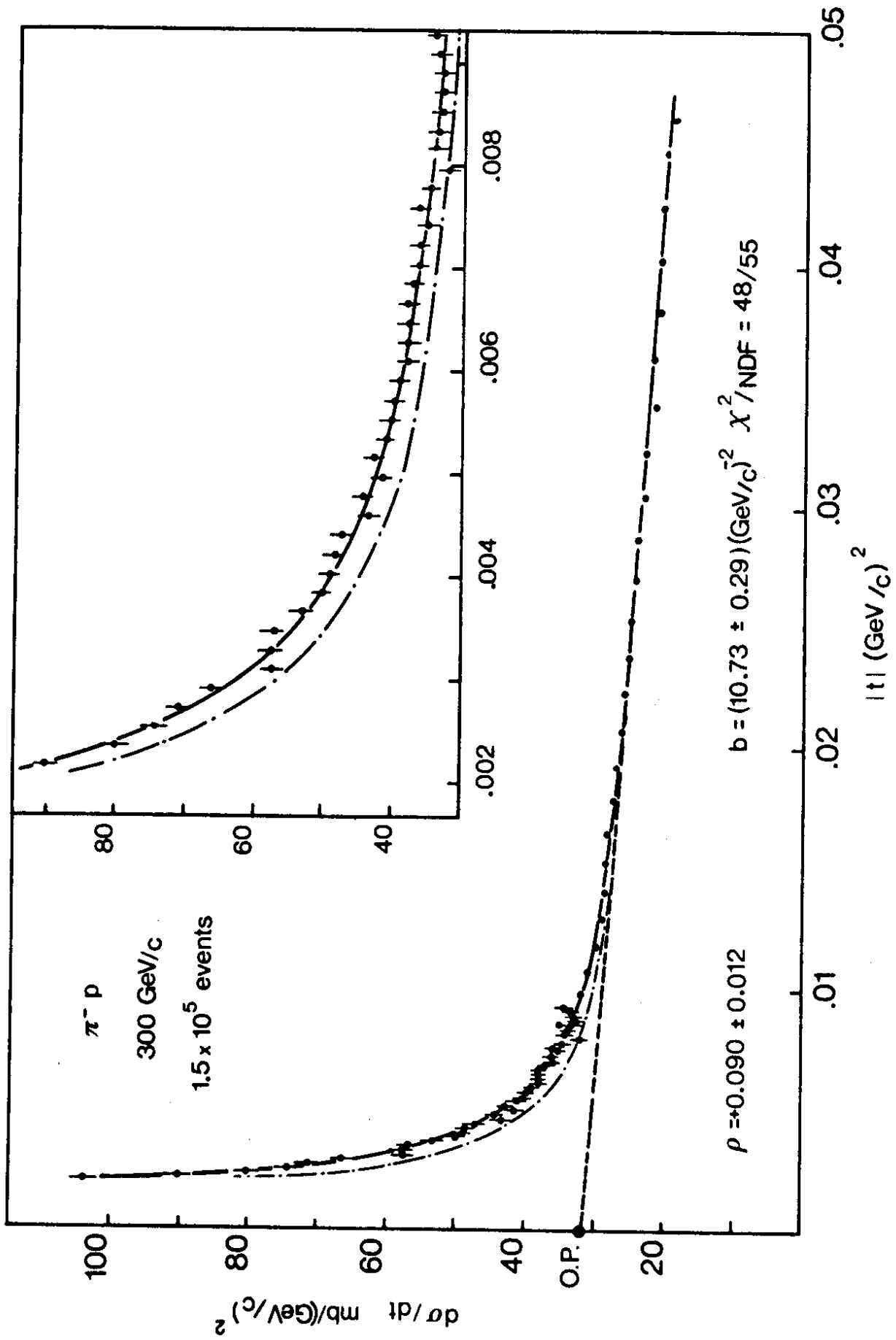


Fig. 1

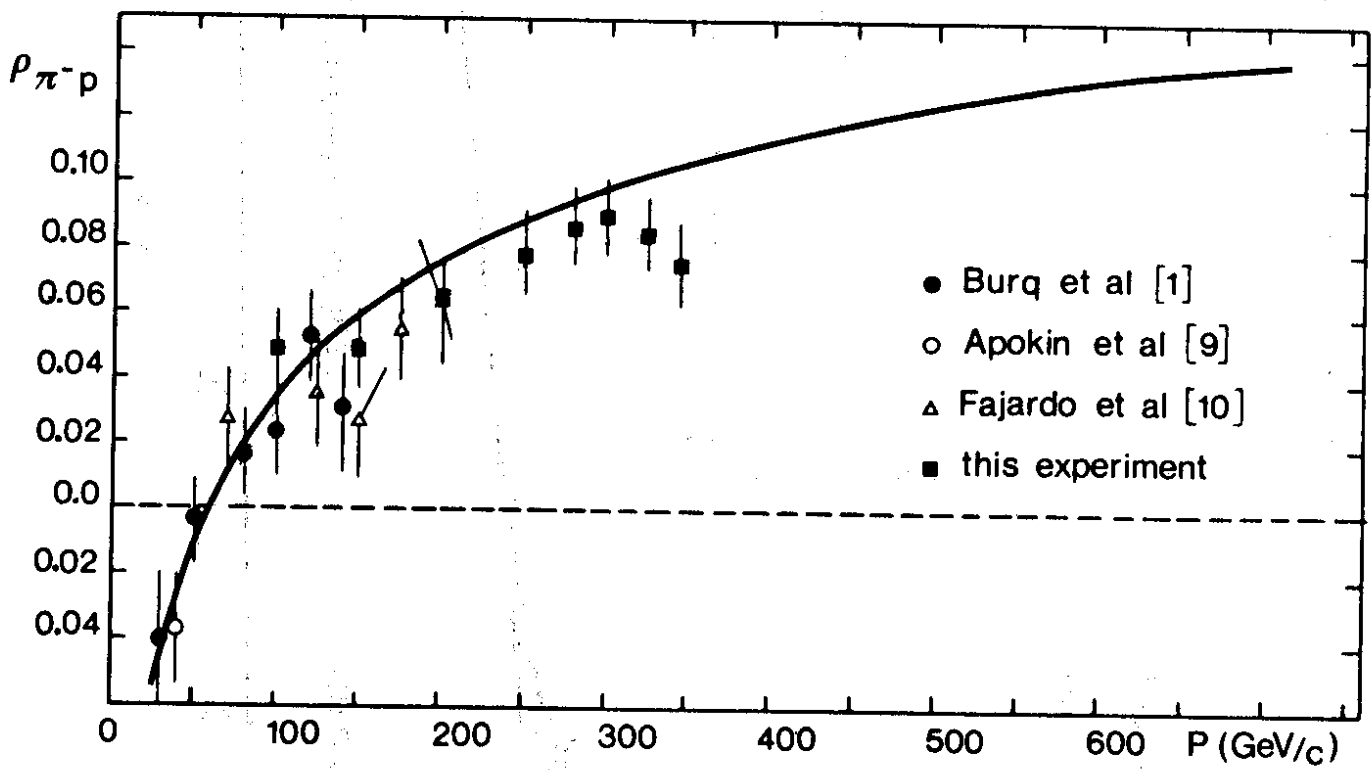


Fig. 2

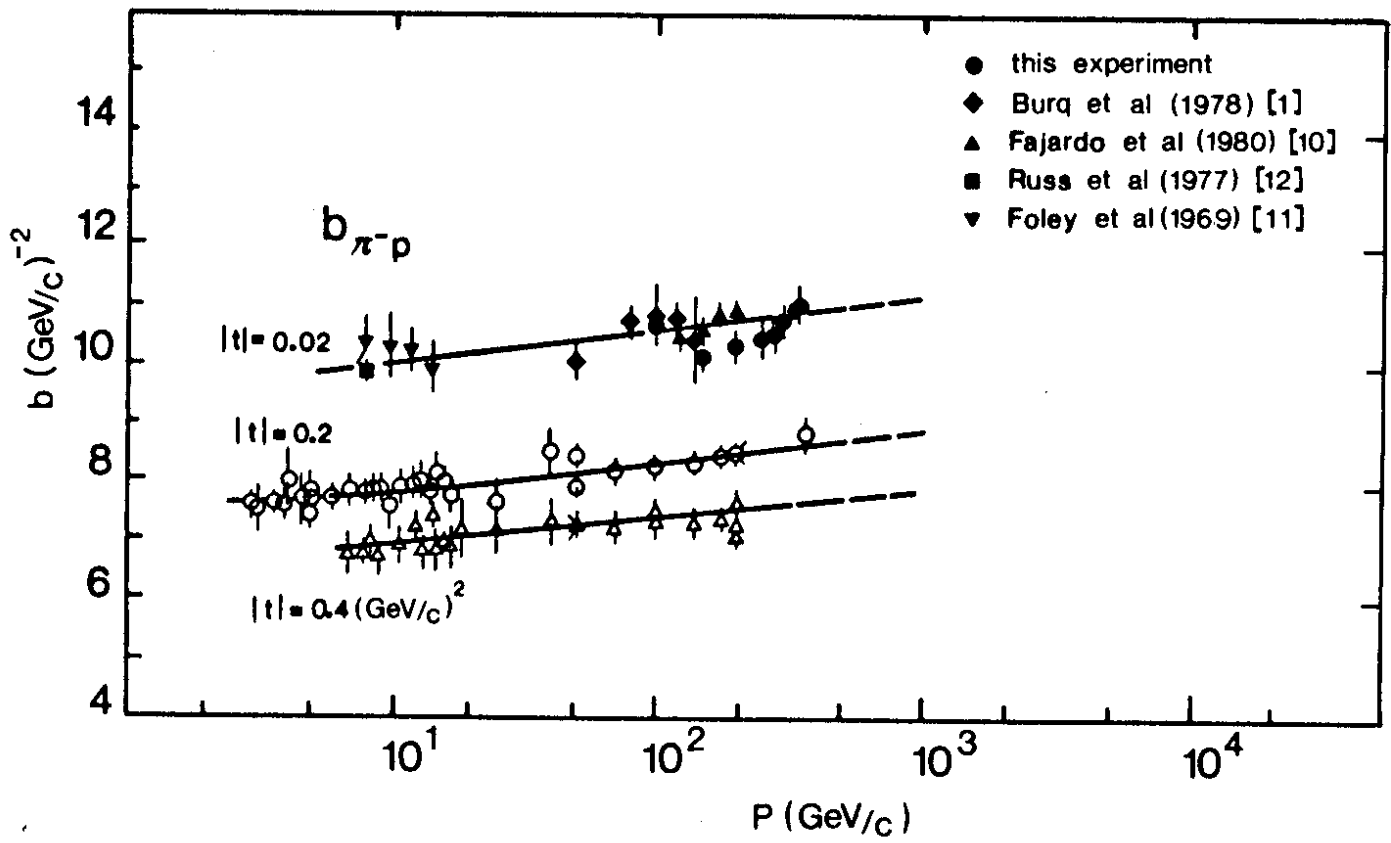


Fig. 3

1

1